FULL-LENGTH ORIGINAL RESEARCH

Comparison of magnetic source estimation to intracranial EEG, resection area, and seizure outcome

*Jeffrey R. Tenney, *Hisako Fujiwara, *†Paul S. Horn, and *Douglas F. Rose

Epilepsia, 55(11):1854–1863, 2014
doi: 10.1111/epi.12822

Dr. Jeffrey Tenney is an assistant professor of Pediatrics and Neurology at Cincinnati Children's Hospital.

Summary

Objectives: **Magnetoencephalography (MEG) is used to guide intracranial electroencephalography (ICEEG) monitoring and determine areas for resection. The purpose of this retrospective cross-sectional study was to report our experience using dipole modeling/dipole scanning, current density reconstructions, and beam-forming methods in a large cohort of pediatric patients with intractable epilepsy.**

Methods: **Source localization results for each algorithm and seizure-onset zone, defined by ICEEG, were described by three blinded reviewers according to five location criteria. The accuracy of each algorithm was then compared to ICEEG. The relationships between the accuracy of these algorithms (discordant, lobar concordant, sublobar concordant) and long-term seizure outcome was calculated using positive and negative predictive values.**

Results: **Thirty-two patients (mean age ± SD, 10.8 ± 5 years) were included in this retrospective review. No algorithms had sublobar concordance with ICEEG in all patients, including when algorithms were grouped by type (dipole modeling/dipole scanning, current density reconstruction, beam forming). Synthetic aperture magnetometry (SAM) with excess kurtosis tended to be the most accurate, but there were no significant differences between algorithms. When comparing the source modeling with ICEEG findings, significantly more patients with a seizure-free outcome were found to have lobar or sublobar concordance of multiple signal classification (MUSIC) (61.1%) and standardized low resolution brain electromagnetic tomography (sLORETA) (52.9%). Positive predictive values were highest for MUSIC (61.9%) and equivalent current dipole (ECD) (57.1%). Negative predictive values were highest for SAM(g_2)-VS (83%), minimum norm estimate (MNE) (75%), MUSIC (73.7%), and ECD (73.5%).**

Significance: **This study describes the use of multiple MEG source estimation techniques and demonstrates that all algorithms have similar rates of concordance with ICEEG. Also, the concordance or discordance of MUSIC with ICEEG was the best predictor of long-term seizure outcome.**

KEY WORDS: **Magnetoencephalography, Epilepsy surgery, Epilepsy.**

Identification of the seizure-onset zone (SOZ) is the primary outcome of presurgical evaluation for patients with medically refractory epilepsy. Resection of the SOZ should render the patient seizure-free, so defining it presurgically is critical.[1] A multimodal noninvasive evaluation can be used to target the location of intracranial electroencephalography (ICEEG) recording and determine the size and extent of the expected resection.[2]

Magnetoencephalography (MEG) is a noninvasive technique that is often used to localize the irritative zone responsible for generating interictal discharges and, presumably, generating seizures.[3] Once the MEG signal is acquired, however, in order to describe the generators of that signal in the brain one must solve the inverse problem.[4] This involves estimating the properties of current sources

Accepted September 2, 2014; Early View publication October 13, 2014.
*Division of Neurology, Cincinnati Children's Hospital Medical Center, Cincinnati, Ohio, U.S.A.; and †Department of Mathematical Sciences, University of Cincinnati, Cincinnati, Ohio,U.S.A.
Address correspondence to Douglas Rose, Division of Neurology, Cincinnati Children's Hospital Medical Center, 3333 Burnet Ave, Cincinnati, OH 45229, U.S.A. E-mail: douglas.rose@cchmc.org

Wiley Periodicals, Inc.

within the brain that could have produced the signals measured by the MEG sensors on the surface.[5] A solution to the inverse problem is typically proposed through the use of various source modeling algorithms.

One of the most commonly used approaches is to model active neurons with an equivalent current dipole (ECD).[6,7] This method of modeling the recorded MEG activity has been found to correlate well with the SOZ as identified with ICEEG.[8,9] It becomes limited, however, if the source is complex and many dipoles are needed. Therefore, scanning methods such as multiple signal classification (MUSIC) were developed, in which a source is estimated by scanning all possible positions in the brain.[10] However, assumptions regarding the identification of signal versus noise are necessary.

Current density models offer an alternative method by limiting the solution space through the placement of large numbers of small current dipoles within the cortex so their strengths can be estimated as a function of time. This results in a minimum norm estimate (MNE) but minimization favors the superficial currents closest to the sensors.[11,12] Standardized low resolution brain electromagnetic tomography (sLORETA) allows postprocessing of the minimum norm results, which improves this superficial source bias and transforms the MEG data into more of a "functional image."[13,14] Further development led to the sLORETA-weighted accurate minimum norm (SWARM), which computes a current density vector field and attempts to provide a low error localization result to the inverse problem.[15]

An additional approach is beamforming, which scans the brain volume by using spatial filters that are optimized to identify specific brain areas with maximal signal while suppressing activity from other areas.[16,17] The most widely used nonlinear adaptive beamformer approach is synthetic aperture magnetometry (SAM).[18] This technique can be advantageous because it requires little user interaction and no a priori information regarding the number of sources. SAM with excess kurtosis (SAM(g_2)) is biased toward detecting infrequent events (i.e., spikes) so that very frequent events may be ignored. SAM can also use the peaks of the kurtosis as virtual sensor locations and provide the resulting reconstructed waveforms (SAM(g_2)-VS). The number of dipole sources is not specified in advance; the assessment of activity by excess kurtosis determines how many "source regions" are present, so the process is independent of examiner bias at this point. Pediatric patients can at times have spikes so frequent that SAM(g_2) will not detect them at all. For this reason we chose virtual sensor locations that were distributed on all the cortical surfaces with 1 cm spacing based on each patient's magnetic resonance imaging (MRI) scan (SAM-VSsym) as an additional method. The virtual sensor locations/orientations are just locations. The same algorithm can be used to reconstruct the time series of signal (virtual sensor waveform) at that location during the recording. Although the locations are chosen objectively based on the statistic of kurtosis and excess kurtosis, the virtual sensor waveforms from each location must be compared to determine which location shows the earliest activity during an interictal discharge and which location has the highest amplitude. These last two steps are very similar to reading the original EEG and MEG signals to determine earliest onset, and requires encephalographer interpretation skills and experience.

Each source modeling algorithm has its own strengths and limitations, but their accuracy for correctly identifying the SOZ is unclear. The purpose of this study was to report our experience using ECD modeling/dipole scanning, current density reconstructions, and beamforming methods in a large cohort of pediatric patients with intractable epilepsy and to determine the accuracy of each algorithm as compared to ICEEG and the resection area. Finally, we report the relationships between the accuracy of these algorithms (discordant, lobar concordant, sublobar concordant) and the long-term seizure outcome.

Materials and Methods

Patients

Data were obtained from patients who underwent MEG recording as part of noninvasive epilepsy surgery evaluation between June 2008 and October 2011. All patients were treated in the epilepsy surgery center at Cincinnati Children's Hospital Medical Center. Inclusion criteria for subjects were as follows: (1) MEG done as part of presurgical evaluation for intractable epilepsy, (2) all source algorithm types completed at the time of data analysis (ECD modeling/dipole scanning, current density reconstruction, and beamforming), (3) ICEEG monitoring with grid electrodes to identify the seizure-onset zone, and (4) resective epilepsy surgery completed. Exclusion criteria for a MEG study were as follows: (1) limited MEG analysis, (2) only ictal MEG recorded, (3) ICEEG with no seizures recorded, and (4) hemispherotomy procedure.

Extensive presurgical evaluation was performed as part of the selection process for potential surgery and has been described previously in detail.[2] In brief, our standard presurgical evaluation included detailed history and clinical examination, scalp video–electroencephalogram (EEG) monitoring, magnetic resonance imaging (MRI), 2-deoxy-2-(18F)fluoro-D-glucose PET (FDG-PET), ictal/interictal single photon emission computed tomography (SPECT), and MEG. ICEEG was used for further localization of the ictal-onset zone and to map eloquent cortices. Clinical decisions regarding surgical candidacy, grid electrode placement, and resection plan were made with multidisciplinary input on the basis of all available data. In relation to our current study, the location of all MEG source estimations were reanalyzed by three independent reviewers.

MEG recording

MEG was recorded with a whole head CTF 275-channel MEG system (VSM MedTech Systems Inc., Coquitlam, BC, Canada) with sampling rates of 300 or 600 Hz and 4,000 Hz for 10- and 2-min recordings, respectively, for a total of at least 40 min for each patient. Scalp-EEG was recorded simultaneously at the same settings as MEG using the VSM MedTech system with 23 scalp electrodes placed according to the International 10-20 system and an additional electrocardiogram (ECG) electrode. For each patient, three fiducial points at the nasion and left and right preauricular locations were marked with a pen and photographed. Fiducial sources (head coils) were then placed at the three locations. Head position relative to the magnetometer array was assessed at the beginning and end of each recording segment using the head coils with the CTF head localization software for 300 and 4,000 Hz sampling rate dataset. Continuous head localization was applied for the 600 Hz sampling rate datasets. Only recordings with <5 mm head movement were accepted.

MEG data analysis

All the original simultaneous EEG and MEG recordings were first visually reviewed for interictal epileptiform discharges. Sections of the recording with muscle artifact were identified by visual inspection and excluded from further analysis. Individual spikes were identified in sections of the simultaneous EEG/MEG signals using Curry 6 (Compumedics Neuroscan, Charlotte, NC, U.S.A.). The particular frequency bandwidth was chosen after first reviewing the power spectrum using short-time Fourier transform of each event in a wide bandwidth and then stepwise narrowing the bandwidth to better discern the frequency of the earliest spectral power change. Principal component analysis followed by independent component analysis was applied to evaluate the possible number of components in each spike signal above the background noise level. The analysis time range was selected at the onset of MEG interictal spikes in order to have sufficient data sampled and signal-to-noise ratio required for the algorithms, while limiting source localization to the earliest activity in the epileptiform discharges.

The realistic volume conductor model was created from each patients' individual MRI automatically or manually as a three-compartment boundary element model;[19] an anatomically constrained linear estimation approach was applied, assuming the sources were distributed in the cerebral cortex.[20]

MEG source estimation

The multiple source estimation methods applied to MEG recordings included ECD, MUSIC, MNE, sLORETA, and SWARM. Also, beamformer localization methods were used including SAM(g_2), SAM(g_2)-VS, and SAM-VSsym. These were performed using CTF software functions (Port Coquitlam, BC, Canada). The initial SAM(g_2) analyses were completed using bandpass filters of 20–70 Hz to exclude low frequency activity that would obscure the detection of spike activity. This analysis detected peaks in excess kurtosis that then served as the virtual sensor locations for the SAM(g_2)-VS analysis. For the SAM-VSsym, VS locations were spaced at 1 cm throughout the entire cerebral cortex surface based on each patient's reconstructed three-dimensional MRI scan. The virtual sensor waveform was calculated for each VS location for both the SAM(g_2)-VS and SAM-VSsym methods. Each VS waveform was then compared to the simultaneous original EEG and MEG signals in each recording. Only VS waveforms that occurred simultaneously with identifiable spikes or sharp waves in the original EEG/MEG signals were accepted for further analysis. All spike types and locations identified for a patient were modeled for this analysis. The earliest onset spike in the waveform was chosen as the putative interictal-onset location. An example of the results from these MEG source estimations can be seen in Fig. 1.

Determination of concordance with ICEEG and resection area

The results of the source modeling described earlier were reviewed retrospectively by three individuals trained in MEG source analysis (J.R.T., H.F., D.F.R.), who were blinded to ICEEG results and clinical outcome. The source localization for each algorithm was described according to the following five criteria: (1) left or right hemisphere; (2) frontal, parietal, temporal, occipital, caudate, or insula; (3) medial or lateral; (4) superior, middle, inferior (for sublobar localization); and (5) anterior, middle, posterior (for sublobar localization). ICEEG data were also reviewed retrospectively to determine the location of the SOZ, as defined at the time of the ICEEG recording. Intracranial grid electrode reconstructions from postoperative head computed tomography (CT) scans were coregistered with each patient's brain MRI to determine the precise location of the seizure onset, according to the same criteria used for the source algorithms. The resection area was defined by reviewing the operative reports, intraoperative photographs, and postoperative imaging. The same location criteria used for source estimation and ICEEG was used to define the resection area. Therefore, a "rating" of 5/5 indicated perfect agreement of the five localization parameters between the source estimation and ICEEG/resection area; 4/5 indicated agreement on hemisphere, lobe, mesial/lateral, and one of two sublobar locations; 3/5 indicated agreement on hemisphere, lobe, and mesial/lateral, but neither sublobar location; 2/5 indicated agreement on hemisphere and lobe but not mesial/lateral or either sublobar location; 1/5 indicated agreement on hemisphere but not lobe; 0/5 indicated contralateral findings between source estimation and ICEEG/resection area. Interrater agreement for these five location criteria was determined for the source estimation, ICEEG,

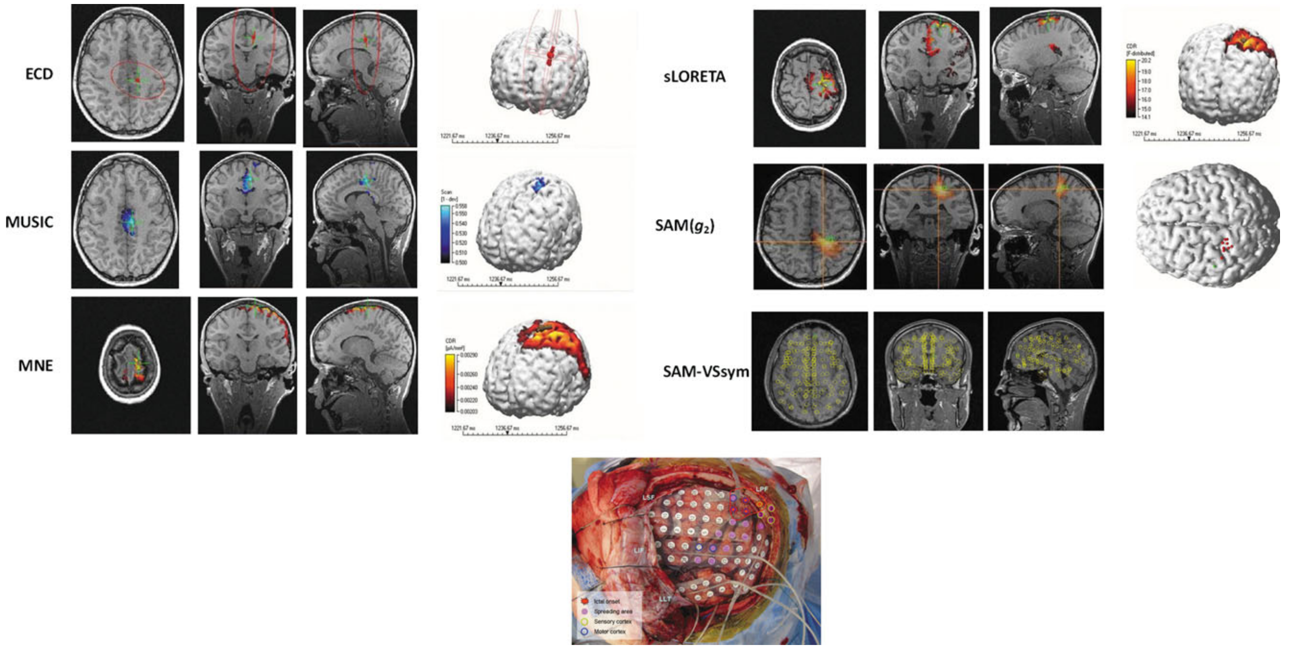

Figure 1.
Example of multiple MEG source estimation algorithms (top) compared to ICEEG (bottom). ECD, MUSIC, MNE, sLORETA, and SAM(g_2) show source estimation results on axial, coronal, and sagittal planes as well as overlaid on a three-dimensional brain reconstruction. The confidence halo surrounding the ECD dipole result is used to symbolize its reliability. The size of its axes is inversely proportional to the signal-to-noise ratio of the measured data.[27] SAM-VSsym shows the distribution of bilaterally symmetrical virtual sensors that were used. ICEEG results for the same patient are shown in the bottom panel where the ictal onset (red) and ictal spread (pink) areas can be seen as well as the results of sensory (green) and motor (blue) extraoperative mapping results.
Epilepsia © ILAE

and resection findings and was assessed using a univariate analysis (a one-sided z-test because the sample size was reasonably large, approximately 80). Those locations lacking agreement among the reviewers were re-reviewed jointly so that a collaborative decision could be made.

Comparison of the source algorithm localization with the SOZ, based on ICEEG, and the resection area was completed for each epileptiform discharge. The accuracy of each algorithm was based on a five-point scale (same as that used to describe the locations) to determine concordance with ICEEG and resection area results: sublobar concordance (4/5 or 5/5—matched on side, lobe, mesial/lateral, and sublobar location), lobar concordance (2/5 or 3/5—matched on side and lobe), discordant (1/5—matched only to same side), or contralateral (0/5—contralateral results). Each algorithm was evaluated separately and then grouped by type of algorithm as follows: ECD modeling/dipole scanning (ECD + MUSIC), current density reconstruction (MNE + sLORETA + SWARM), and beamforming (SAM (g_2), SAM(g_2)-VS, SAM-VSsym.

Source algorithm accuracy and seizure outcome

The seizure outcome for each patient was based on a Cincinnati Children's Hospital epilepsy surgery database query and chart reviews of clinic notes at 24 months postsurgery. Seizure outcome was classified based according to the system proposed by the ILAE: (1) seizure-free with no auras; (2) only auras, no other seizures; (3) one to three seizure days per year; (4) four seizure days per year to 50% reduction of baseline seizure values, (5) <50% reduction of baseline seizure days to 100% increase of baseline seizure days; and (6) >100% increase of baseline seizure days. Fischer's exact test was used to test the association between the source algorithm concordance and ILAE outcome (dichotomized to a good outcome [ILAE = 1] versus a poor outcome [ILAE = 2–6]). Positive and negative predictive values were assessed based on the concordance of each algorithm compared to ICEEG at 24 months of follow-up. The positive predictive values (PPVs) were determined by calculating the proportions of good concordance results (accuracy 3–5) that occurred with seizure-free (ILAE = 1) outcome. Similarly, the negative predictive values (NPVs) were determined by calculating the proportions of discordant results (accuracy 0–2) that occurred with poor (ILAE = 2–6) outcomes. Those cases in which the area of source estimation was not covered by grids for ICEEG were excluded from analysis.

The STROBE criteria were followed in the preparation of this manuscript (Data S1).

Results

Patients

A total of 230 patients had a MEG completed as part of a noninvasive epilepsy surgery evaluation (Fig. 2). There were 55 patients who had all source algorithm types completed as part of the analysis (ECD modeling/dipole scanning, current density reconstruction, and beamforming), and 48 of those underwent ICEEG. There were 32 patients who eventually had a focal cortical resection and were used for all subsequent analyses. The remaining patients were excluded because they had a hemispherotomy (N = 11), prior resection (N = 1), or no resection was completed (N = 4). Patient demographics are listed in Table 1. The mean age of these patients at the time of surgery was 10.8 ± 5 years. The mean duration of epilepsy at the time of surgery was 6.3 ± 3.9 years. The distribution of focal epilepsies included the following: frontal 10/32 (31.3%), parietal 1/32 (3.1%), temporal 8/32 (25%), occipital 1/32 (3.1%), and multifocal 12/32 (37.5%). The temporal epilepsies included mesial temporal 4/8 (50%) and neocortical temporal 4/8 (50%).

Inter-rater agreement

After the locations for source estimation, ICEEG, and resection results were determined independently by each reviewer, the interrater agreement was assessed using a univariate analysis. There was good agreement at the level of sublobar localization for both the SAM(g_2)-VS and all areas of resection (4/5 location parameters) ($p \geq 0.104$). For all other source algorithms and the location of the SOZ using ICEEG, there was good interrater agreement at the level at lobar, but not sublobar localization (3/5 location parameters) ($p \geq 0.15$).

Source algorithm, ICEEG, and resection area concordance

Each source algorithm demonstrated lobar concordance with ICEEG findings (Fig. 3). The rate of sublobar concordance with ICEEG was never >50%, including when algorithms were grouped by type (ECD modeling/dipole scanning, current density reconstruction, beamforming). SAM(g_2) had the highest rate of sublobar concordance (48.8%), and overall the beamforming algorithms had the highest rates of sublobar concordance (43.9%). The rate of discordance was lowest for SAM(g_2)-VS (15%) and highest for SWARM (50%). The SWARM algorithm was significantly less concordant with ICEEG than SAM(g_2), but when the algorithms were grouped by type, the ECD modeling/dipole scanning, current density reconstruction, and beamforming algorithms had fairly equivalent rates of sublobar concordance (36.5%, 36.5%, and 43.9%, respectively).

Higher rates of sublobar concordance were found for each source algorithm location when compared to the location of the resection (Fig. 3). All algorithms had a fairly equivalent degree of accuracy when compared individually to the resection area as well as when grouped by type of source modeling algorithm (75–89.5%).

Source algorithm accuracy and seizure outcome

Source algorithm concordance results were compared in those patients with an ILAE outcome of 1 (seizure-free with no auras) versus those with an ILAE outcome of 2–6 at 24 months postsurgery (Tables 2 and 3, Data S1). When comparing the source modeling results with ICEEG findings, significantly more patients with an ILAE outcome of 1 were found to have lobar or sublobar concordance of MUSIC (61.1%) and sLORETA (52.9%) at 24 month follow-up (Table 2). When algorithms were grouped by type, there was a trend for more

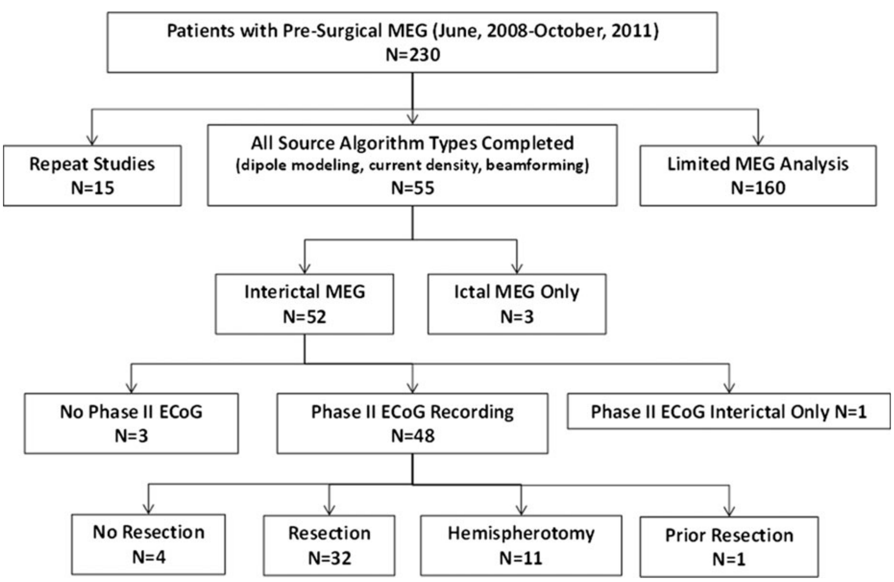

Figure 2.
Flow diagram showing how patients were selected for inclusion in the study. A total of 230 patients had an MEG completed as part of a noninvasive epilepsy surgery evaluation. There were 55 patients who had all source estimation types completed (dipole modeling, current density, and beamforming), and 48 underwent ICEEG recording. There were 32 patients who eventually underwent a focal cortical resection and were used for all subsequent analyses.
Epilepsia © ILAE

Table 1. Patient demographics

Subject no.	Sex	Age at surgery (years)	Duration of epilepsy (years)	Etiology	Presurgical concordance	Surgery location
1	M	17.9	5.9	FCD	Nonlesional concordant	RT
2	F	9.0	8.0	FCD	Nonlesional concordant	LF
3	M	13.2	10.2	Infectious, FCD	Lesional discordant	LT
4	F	10.9	9.4	Vascular	Lesional concordant	ML
5	M	8.6	1.6	FCD	Lesional discordant	LF
6	M	4.2	3.9	TSC	Multilesional discordant	ML
7	M	16.2	16.2	Vascular	Lesional concordant	ML
8	M	17.7	10.7	Neoplastic	Multilesional concordant	ML
9	M	9.1	8.6	TSC	Multilesional concordant	LT
10	F	9.1	3.1	FCD	Lesional concordant	LT
11	M	17.9	8.9	FCD	Nonlesional concordant	ML
12	M	17.7	5.7	FCD	Lesional concordant	RP
13	M	12.7	11.7	Vascular	Lesional discordant	RF
14	M	2.7	2.1	FCD	Lesional concordant	LT
15	M	15.2	14.2	FCD	Lesional concordant	ML
16	F	1.8	0.2	TSC	Multilesional concordant	RO
17	M	3.9	3.6	TSC	Multilesional concordant	LF
18	F	8.0	6.0	FCD	Lesional concordant	RF
19	F	5.8	3.3	FCD	Nonlesional discordant	ML
20	M	9.8	3.6	FCD	Lesional discordant	ML
21	F	10.9	9.3	Unknown	Nonlesional concordant	LF
22	F	6.1	4.7	FCD	Lesional concordant	RF
23	F	6.0	6.0	FCD	Lesional concordant	ML
24	M	11.2	2.2	FCD	Lesional concordant	LT
25	F	13.3	2.3	FCD	Nonlesional concordant	ML
26	M	16.4	3.4	FCD	Nonlesional discordant	LF
27	F	2.1	1.6	TSC	Multilesional discordant	LT
28	F	15.2	3.2	FCD	Nonlesional concordant	RF
29	F	15.2	6.2	Neoplastic, FCD	Lesional concordant	ML
30	M	11.0	9.1	FCD	Nonlesional discordant	LF
31	M	15.7	9.7	FCD	Nonlesional discordant	LT
32	F	12.2	6.2	FCD	Lesional concordant	ML
Average ± SD		10.8 ± 5	6.3 ± 3.9			

Each of the 32 subjects included for analysis are listed along with their sex, age at surgery, duration of epilepsy, etiology (based on pathology diagnosis), presurgical concordance (of electrophysiology and imaging studies), and the location of surgery.

M, male; F, female; FCD, focal cortical dysplasia; TSC, tuberous sclerosis complex; LF, left frontal; LT, left temporal; ML, multilobar; RF, right frontal; RO, right occipital; RP, right parietal; RT, right temporal.

patients with an ILAE outcome of 1 to have lobar or sublobar concordance when ECD modeling/dipole scanning, current density reconstruction, and beamforming algorithms were compared to ICEEG findings at 24 months. In general, when MEG was discordant with ICEEG the rate of a seizure-free outcome was lower.

When comparing the results of source localization to the area of resection, most patients had sublobar concordance (Data S1). This was possibly due to the extensive nature of many resections (i.e., lobectomies). Those times when source localization was discordant with the area of resection were still associated with a high number of seizure-free outcomes, in most cases. This may be related to the influence of other presurgical testing or clinical decision making which disregarded a discordant MEG finding.

Positive and negative predictive values were used to determine how well concordance (accuracy 3–5) or discordance (accuracy 0–2) of source algorithm results with the SOZ (ICEEG) could predict a seizure-free (ILAE = 1) or non–seizure-free (ILAE = 2–6) outcome (Table 3). The positive predictive values were highest for MUSIC (61.9%) and ECD (57.1%). Negative predictive values were highest for SAM(g_2)-VS (83%), MNE (75%), MUSIC (73.7%), and ECD (73.5%). In general, the algorithms had better negative than positive predictive value. When grouped by type of algorithm, the ECD modeling/dipole scanning algorithms had better positive (59.3%) and negative (75%) predictive values than either the current density or beamforming algorithms.

Additional combinations of source algorithms were investigated as well, but there were no significant differences in accuracy, PPV, or NPV, so the results were not included in the tables provided. Likewise, results were dichotomized to evaluate patients with unilateral versus bilateral interictal discharges and extratemporal versus temporal resections. These subgroup results did not differ significantly from those we obtained during the analysis with all patients included.

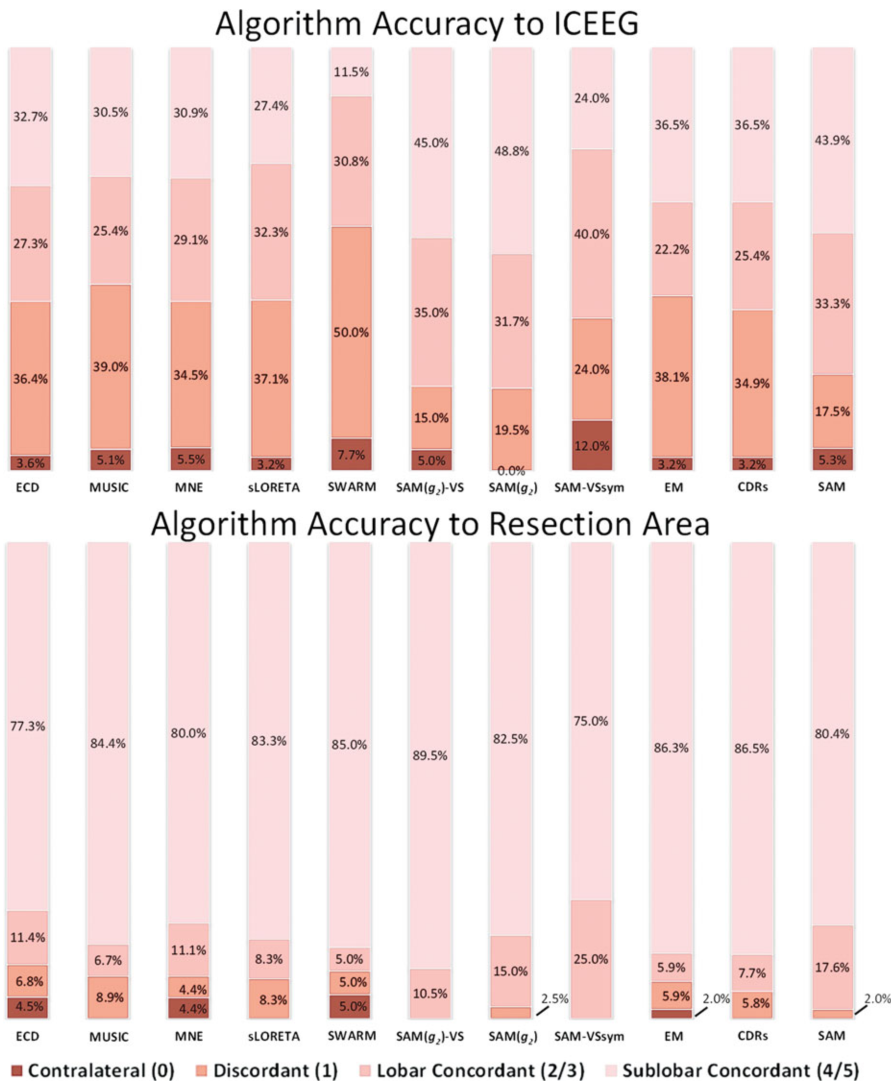

Figure 3.
Source algorithm accuracy compared to ICEEG (top) and the resection area (bottom). Source localization, ictal onset (ICEEG), and the resection area were characterized based on five location parameters. These were then compared to determine concordance (0 = contralateral, 1 = discordant, 2/3 = lobar concordance, 4/5 = sublobar concordance). EM – ECD + MUSIC, CDRs – MNE + sLORETA + SWARM, SAM – SAM (g_2)-VS + SAM(g_2) + SAM-VSsym.
Epilepsia © ILAE

Discussion

The goal of this retrospective study was to describe and compare the localizing value of multiple types of MEG source estimations in pediatric patients with medically refractory epilepsy who require ICEEG evaluation prior to resective epilepsy surgery. We determined the accuracy of each algorithm compared to the SOZ, identified with ICEEG, and the location of the resection. Also, we investigated how the accuracy of each algorithm was related to the long-term seizure outcome. Although there are some studies comparing the results of MEG source estimation to ICEEG, no prior study has assessed the usefulness of these various source estimation techniques. To our knowledge, this is the first study to describe and compare the usefulness of ECD, MUSIC, MNE, sLORETA, SWARM, and various beamforming methods (SAM(g_2)-VS, SAM(g_2), SAM-VSsym) to the current "gold standard" (ICEEG) and the long-term seizure outcome in this population.

The most significant finding from our study is that the accuracy of all these algorithms, despite their differing approaches to solving the inverse problem and their individual strengths and limitations, are relatively similar when compared to ICEEG and the resection area. The exception was the SWARM algorithm, which was found to be significantly less accurate than SAM(g_2), when compared to ICEEG. However, this could be related to our recent implementation of SWARM and therefore smaller sample size. In addition, one should note that source localizations of interictal discharges on MEG were compared to ictal-onset zones recorded with ICEEG. This could potentially explain some of the differences seen in our accuracy measurements.

Another important finding from this study is that the ECD modeling/dipole scanning algorithms (ECD + MUSIC) were better able to predict both seizure-free (ILAE = 1) and non–seizure-free (ILAE = 2–6) outcomes at 24 months based on their concordance and discordance with ICEEG than either the current density reconstruction (MNE + sLO-

Table 2. Source algorithm concordance with ICEEG in relation to postsurgical seizure outcome at 24 months

		ICEEG		
		24 month f/u		
Algorithm	Outcome	Discordant (%)	Lobar concordance (%)	Sublobar concordance (%)
ECD	ILAE = 1	6 (27.3)	5 (41.7)	9 (50)
	ILAE > 1	16 (72.7)	7 (58.3)	9 (50)
MUSIC	ILAE = 1	7 (25.9)	5 (33.6)	11 (61.1)
	ILAE > 1	20 (74.1)	10 (66.6)	7 (38.9)
MNE	ILAE = 1	5 (22.7)	6 (37.5)	8 (47.1)
	ILAE > 1	17 (77.3)	10 (62.5)	9 (52.9)
sLORETA	ILAE = 1	7 (28)	8 (40)	9 (52.9)
	ILAE > 1	18 (72)	12 (60)	8 (47.1)
SWARM	ILAE = 1	5 (33.3)	1 (12.5)	2 (66.6)
	ILAE > 1	10 (66.6)	7 (87.5)	1 (33.3)
SAM(g_2)-VS	ILAE = 1	0 (0)	1 (14.3)	5 (55.6)
	ILAE > 1	4 (100)	6 (85.7)	4 (44.4)
SAM(g_2)	ILAE = 1	5 (62.5)	6 (46.2)	11 (55)
	ILAE > 1	3 (37.5)	7 (53.8)	9 (45)
SAM-VSsym	ILAE = 1	4 (44.4)	2 (20)	2 (33.3)
	ILAE > 1	5 (55.6)	8 (80)	4 (66.6)
EM	ILAE = 1	7 (26.9)	5 (35.7)	13 (56.5)
	ILAE > 1	19 (73.1)	9 (64.3)	10 (43.5)
CDRs	ILAE = 1	7 (29.2)	6 (37.5)	12 (52.2)
	ILAE > 1	17 (70.8)	10 (62.5)	11 (47.8)
SAM	ILAE = 1	7 (53.8)	6 (31.6)	13 (52)
	ILAE > 1	6 (46.2)	13 (68.4)	12 (48)

Concordance was based on the comparison of MEG source localization and ictal onset (determined with ICEEG) (0/1 = discordant, 2/3 = lobar concordance, 4/5 = sublobar concordance). Outcome was dichotomized to look at seizure-free outcomes (ILAE = 1) versus all other outcomes (ILAE = 2–6).
*$p < 0.05$, EM – ECD + MUSIC, CDRs – MNE + sLORETA + SWARM, SAM – SAM(g_2)-VS + SAM(g_2) + SAM-VSsym.

Table 3. Positive and negative predictive values (PPVs, NPVs) for a seizure-free outcome (ILAE = 1) at 24 months when source estimation results are concordant with ICEEG

		24 months	
Algorithm	N	PPV (%)	NPV (%)
ECD	55	57.1	73.5*
MUSIC	59	61.9	73.7*
MNE	55	47.8	75
sLORETA	62	53.8	72.2
SWARM	26	40	71.4
SAM(g_2)-VS	20	45.5	88.9*
SAM(g_2)	41	50	41.2
SAM-VSsym	25	33.3	68.8
EM	63	59.3	75*
CDRs	63	51.7	70.6
SAM	57	46.9	56

PPV indicates how often concordance (accuracy 3–5) predicts a seizure-free (ILAE = 1) outcome. NPV indicates how often discordance (accuracy 0–2) predicts a poor outcome (ILAE 2–6). N, number of interictal discharges analyzed.
*$p < 0.05$, EM – ECD + MUSIC, CDRs – MNE + sLORETA + SWARM, SAM – SAM(g_2)-VS + SAM(g_2) + SAM-VSsym.

RETA + SWARM) or beamforming (SAM(g_2)-VS + SAM (g_2) + SAM-VSsym) methods. However, individual algorithms showed variability in the PPV and NPV, indicating that a combination of algorithms might provide the best prediction of outcome.

It has previously been shown that MEG is a useful tool to localize the SOZ and determine the location of invasive intracranial monitoring and surgical resection. In addition, sublobar concordance of ECD results and ICEEG has been shown to predict a seizure-free outcome in lesional and nonlesional epilepsy surgery patients.[9,21–24] Most of these studies have employed the ECD modeling algorithm exclusively, but more recently, comparisons of various source estimation types have been reported. Zhang et al.[25] evaluated patients with lesional and nonlesional epilepsy using ECD and SAM(g_2) and showed that seizure-free outcomes were higher when MEG findings were concordant with ICEEG. Specifically, there was good agreement between SAM(g_2) and ECD results, although the exact concordance rates for each algorithm were not reported. de Gooijer-van de Groep et al.[26] recently compared interictal MEG spikes using MUSIC, SAM(g_2), and sLORETA to interictal discharges recorded with ICEEG. It was reported that these three MEG methods showed similar concordance with ICEEG but differed depending on the brain region in which the spike was located. Combining MUSIC and SAM (g_2) gave the best results with a PPV of 82%. It is difficult to interpret our results in light of this study as we compared interictal MEG spikes to ictal-onset recorded with ICEEG.

Several limitations of our study should be reviewed. First, this is a single center study with a relatively large cohort of 32 patients, but as subgroup analysis was completed, limited statistical validity and the possibility of type 2 statistical errors should be considered. Comparing our study to larger cohorts of specific pediatric populations, such as patients with nonlesional frontal lobe epilepsy, may strengthen our findings and should be considered as a future study. Second, we included in our MEG analysis all interictal discharges that were recorded for a particular patient, even if they occurred rarely or were not the predominant type. This may artificially worsen our rates of concordance, since the clinical decisions of where to place invasive recording electrodes and complete the resection may have been based on the predominant spike type and concordance of multimodality presurgical testing. Future studies that exclude rare spikes occurring outside of the predominant spike location may help to strengthen the findings. In addition, because we excluded those algorithm results that could not be verified by ICEEG (not covered by the grid electrodes), the results we present may overestimate the overall accuracy of source estimations of MEG. Finally, since each type of source estimation is known to have its own strengths and limitations, in clinical practice the use of these multiple algorithms is influenced by the location of interictal discharges that are recorded. As such, if spikes are very frequent, less weight will be given to beamforming methods such as SAM(g_2) and SAM(g_2)-VS, since these may ignore very frequent events. Similarly, if an interictal discharge is thought to originate in a deep structure, such as the hippocampus, then MNE would not be optimal because it is biased toward localizing superficial sources. Therefore, the results of our study are limited, since the clinical use of these algorithms can be influenced by these factors. Future studies that place interictal discharges into subgroups, such as infrequent spikes or mesial spikes, might be more clinically relevant. In addition, the effect of using multiple types of source estimation, such as ECD modeling/dipole scanning + beamforming or current density reconstruction + beamforming, should be considered because this may maximize the strengths and limit the weaknesses of the individual algorithms.

Despite these limitations, this study describes our experience using these multiple types of MEG source estimation to provide presurgical localization and demonstrates that all algorithms have similar rates of concordance with ICEEG and the area of resection. This is despite the fact that it is well known that each algorithm has its own strengths and limitations. Also, the concordance or discordance of ECD modeling/dipole scanning algorithms, such as ECD and MUSIC, with ICEEG were the best predictors of long-term seizure outcome in a population of pediatric patients who underwent resective epilepsy surgery. It is our hope that these findings will drive further research to optimize the use of MEG as a noninvasive, presurgical tool.

Acknowledgment

We would like to thank Hans Greiner, MD, for his thoughtful review of this manuscript.

Disclosure

None of the authors has any conflict of interest to disclose. We confirm that we have read the Journal's position on issues involved in ethical publication and affirm that this report is consistent with those guidelines.

References

1. Rosenow F, Luders H. Presurgical evaluation of epilepsy. *Brain* 2001;124(Pt 9):1683–1700.
2. Seo JH, Holland K, Rose D, et al. Multimodality imaging in the surgical treatment of children with nonlesional epilepsy. *Neurology* 2011;76:41–48.
3. Grondin R, Chuang S, Otsubo H, et al. The role of magnetoencephalography in pediatric epilepsy surgery. *Childs Nerv Syst* 2006;22:779–785.
4. Darvas F, Pantazis D, Kucukaltun-Yildirim E, et al. Mapping human brain function with MEG and EEG: methods and validation. *Neuroimage* 2004;23(Suppl 1):S289–S299.
5. Grech R, Cassar T, Muscat J, et al. Review on solving the inverse problem in EEG source analysis. *J Neuroeng Rehabil* 2008;5:25.
6. Fuchs M, Wagner M, Wischmann HA, et al. Improving source reconstructions by combining bioelectric and biomagnetic data. *Electroencephalogr Clin Neurophysiol* 1998;107:93–111.
7. Scherg M, Berg P. Use of prior knowledge in brain electromagnetic source analysis. *Brain Topogr* 1991;4:143–150.
8. Agirre-Arrizubieta Z, Huiskamp GJ, Ferrier CH, et al. Interictal magnetoencephalography and the irritative zone in the electrocorticogram. *Brain* 2009;132(Pt 11):3060–3071.
9. Schneider F, Alexopoulos AV, Wang Z, et al. Magnetic source imaging in non-lesional neocortical epilepsy: additional value and comparison with ICEEG. *Epilepsy Behav* 2012;24:234–240.
10. Mosher JC, Lewis PS, Leahy RM. Multiple dipole modeling and localization from spatio-temporal MEG data. *IEEE Trans Biomed Eng* 1992;39:541–557.
11. Fuchs M, Wagner M, Kohler T, et al. Linear and nonlinear current density reconstructions. *J Clin Neurophysiol* 1999;16:267–295.
12. Wang JZ, Williamson SJ, Kaufman L. Magnetic source imaging based on the minimum-norm least-squares inverse. *Brain Topogr* 1993;5:365–371.
13. Pascual-Marqui RD, Michel CM, Lehmann D. Low resolution electromagnetic tomography: a new method for localizing electrical activity in the brain. *Int J Psychophysiol* 1994;18:49–65.
14. Wagner M, Fuchs M, Kastner J. Evaluation of sLORETA in the presence of noise and multiple sources. *Brain Topogr* 2004;16:277–280.
15. Wagner M, Fuchs M, Kastner J. SWARM: sLORETA-weighted accurate minimum norm inverse solutions. *Int Congr Ser* 2007;1300:185–188.
16. Hillebrand A, Barnes GR. Beamformer analysis of MEG data. *Int Rev Neurobiol* 2005;68:149–171.
17. van Veen BD, Buckley. Beamforming: a versatile approach to spatial filtering. *IEEE ASSP Magazine* 1988;5:4–24.
18. Kirsch HE, Robinson SE, Mantle M, et al. Automated localization of magnetoencephalographic interictal spikes by adaptive spatial filtering. *Clin Neurophysiol* 2006;117:2264–2271.
19. Fuchs M, Wagner M, Kastner J. Boundary element method volume conductor models for EEG source reconstruction. *Clin Neurophysiol* 2001;112:1400–1407.
20. Dale AM, Sereno MI. Improved localizadon of cortical activity by combining EEG and MEG with MRI cortical surface reconstruction: a linear approach. *J Cogn Neurosci* 1993;5:162–176.
21. Knowlton RC, Elgavish RA, Bartolucci A, et al. Functional imaging: II. Prediction of epilepsy surgery outcome. *Ann Neurol* 2008;64:35–41.

22. Knowlton RC, Elgavish RA, Limdi N, et al. Functional imaging: I. Relative predictive value of intracranial electroencephalography. *Ann Neurol* 2008;64:25–34.
23. Huiskamp G, Agirre-Arrizubieta Z, Leijten F. Regional differences in the sensitivity of MEG for interictal spikes in epilepsy. *Brain Topogr* 2010;23:159–164.
24. Knowlton RC, Razdan SN, Limdi N, et al. Effect of epilepsy magnetic source imaging on intracranial electrode placement. *Ann Neurol* 2009;65:716–723.
25. Zhang R, Wu T, Wang Y, et al. Interictal magnetoencephalographic findings related with surgical outcomes in lesional and nonlesional neocortical epilepsy. *Seizure* 2011;20(9):692–700.
26. de Gooijer-van de Groep KL, Leijten FS, Ferrier CH, et al. Inverse modeling in magnetic source imaging: comparison of MUSIC, SAM (g2), and sLORETA to interictal intracranial EEG. *Hum Brain Mapp* 2013;34:2032–2044.
27. Fuchs M, Wagner M, Kastner J. Confidence limits of dipole source reconstruction results. *Clin Neurophysiol* 2004;115:1442–1451.

Supporting Information

Additional Supporting Information may be found in the online version of this article:

Data S1. Source algorithm concordance with the resection area in relation to postsurgical seizure outcome at 24 months.